Transient pull-in simulation of electrostatic microvalve with physics-based contact function

Grim Keulemans[a], Boshen Liang[a,b], Alexey Podkovskiy[a], Shruti Jambaldinni[a], Dominika Wysocka[a], Lei Zhang[a], Tim Stakenborg[a], David Cheyns[a], Paul Heremans[a,b], Veronique Rochus[a]

[a]imec, Kapeldreef 75, Leuven, B-3001, Belgium
[b]KU Leuven, Leuven, Belgium

grim.keulemans@imec.be, tel. +32 16 287560

Abstract

We report the fluid-structure interaction (FSI) modeling of an electrostatic actuated gas modulating microvalve. A physics-based contact function was introduced, with improved stability compared to pure penalty and augmented Lagrangian. The valve position and the transient gas flux at the inlet and outlet of the valve during the pull-in and snap-out events were simulated, showing voltage hysteresis and distinct flow patterns between the two events.

1. Introduction

The prediction of the transient behavior of electrostatic valves with the finite-element (FE) method is challenging, nonetheless important when the valve is embedded in a larger fluidic platform (time and position dependent pressure levels, crosstalk, ...) [1]. The deflection of the valve membrane is typically larger than the thickness of the membrane, meaning geometric and material nonlinearity (hyperelasticity) needs to be considered. Also, the electrostatic force-displacement relationship is nonlinear. When the voltage between the electrode on the flexible membrane and the ground electrode at the bottom of the channel reaches a critical value, i.e. pull-in voltage, the membrane collapses on the ground electrode.

The rapidly deforming mesh of the fluidic domain makes convergence difficult to obtain. Tricks to achieve stable solutions by fixing the displacement at the center of the membrane and solving for the voltage that generates this displacement by means of a root finding algorithm, as proposed in [2], are acceptable for steady state problems but become inadequate for transient simulations.

To avoid inverted mesh elements during one of the Newton iterations of the nonlinear FE solver, a proper contact function must be added to the FE formulation. Standard contact models available in commercial FE packages such as Comsol Multiphysics and Ansys Mechanical, i.e. pure penalty and augmented Lagrangian, are difficult to set up.

The contact pressure t_p of the pure penalty method can be expressed as [3]:

$$t_p = \begin{cases} -k_p d_g + p_0 & \text{if } d_g < p_0/k_p \\ 0 & \text{if } d_g \geq p_0/k_p \end{cases} \quad (1)$$

d_g is the effective gap distance. p_0 represents the contact pressure at zero gap. The penalty factor k_p can be interpreted as the stiffness of contact. A high k_p fulfills the contact condition more accurately. If however k_p is too high, the model becomes ill-conditioned and unstable. As a consequence, the coefficients of the pure penalty method (k_p and p_0) must be adapted for each change in geometry and/or boundary condition (e.g. voltage ramp rate, backpressure due to the gas flow in the microchannel). The augmented Lagrangian method is less sensitive to the magnitude of the (user) pre-defined stiffness compared to the pure penalty method. The Lagrange term λ_m augments the contact pressure calculation [3]:

$$t_{np} = \begin{cases} \lambda_m - k_p d_g & \text{if } d_g \leq 0 \\ \lambda_m e^{-\frac{k_p d_g}{\lambda_m}} & \text{otherwise} \end{cases} \quad (2)$$

The disadvantage of the augmented Lagrangian method for electrostatic pull-in modeling is that it requires a lot of damping, making the simulations time consuming. Here, we introduce a convenient physics-based contact function with improved stability.

2. Theory

To explain the principle of the physics-based contact function, the electrostatic microvalve is simplified as a parallel-plate capacitor separated by an initial gap g, as shown in Figure 1. The top or movable electrode represents the membrane. Its deflection stiffness is defined by the attached spring with a spring constant k_{mech} derived based on the Kirchhoff-Love plate theory (normalized to area) [4]:

$$k_{mech} = \frac{64\,D}{a^4} \text{ with } D = \frac{Et^3}{12(1-\nu^2)} \quad (3)$$

In Eq. (3), a represents the membrane radius, t the membrane thickness and D the flexural rigidity of the membrane. E and ν are respectively the elastic modulus and Poisson's ratio of the membrane material.

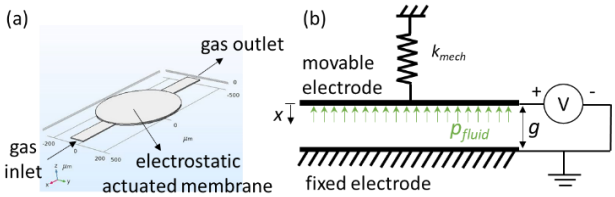

Figure 1: (a) Electrostatic actuated gas modulating microvalve; (b) Equivalent parallel-plate capacitor model

By applying a voltage V between the top (valve membrane) and fixed bottom electrode (valve floor), the resulting electrostatic force causes the membrane to move towards the ground electrode. The electrostatic force as

function of the valve membrane displacement x of can be expressed as (again normalized to area) [5]:

$$p_{el}(x,V) = \frac{\varepsilon V^2}{2(g-x)^2} \quad (4)$$

with ε the permittivity of the gas and g the initial gap between the electrodes.

When gas is flowing through the valve structure, a net pressure p_{fluid} will be present in the valve cavity, pushing the membrane upwards. The net pressure balance of electrostatic valve structure can therefore be written as:

$$p_{tot}(x,V) = p_{el}(x,V) - p_{mech}(x) - p_{fluid} = \frac{\varepsilon V^2}{2(g-x)^2} - k_{mech}x - p_{fluid} \quad (5)$$

At equilibrium, the electrostatic, mechanical, and fluid pressures will cancel each other ($p_{tot}(x) = 0$) and Eq. (5) can be solved for the valve position x as function of the applied voltage V. However, when a critical voltage is achieved, the electric pressure ($\sim 1/(g\text{-}x)^2$) becomes dominant with respect to the mechanical and fluid pressure ($\sim x$) and the valve membrane collapses on the valve floor. This critical voltage is called the *pull-in voltage* and occurs when $dp_{tot}(x,V)/dx = 0$, i.e. the electro-mechanical system has zero stiffness. The analytical expression for the pull-in voltage V_{pi} and the corresponding displacement x_{pi} are (ignoring the fluid pressure, i.e. $p_{fluid} \approx 0$) [5]:

$$V_{pi} = \sqrt{\frac{8}{27}\frac{k_{mech}g^3}{\varepsilon}} \text{ and } x_{pi} = \frac{1}{3}g \quad (6)$$

By integration, the energy balance of the electrostatic valve structure can be derived (normalized to area):

$$e_{tot}(x,V) = e_{el}(x,V) - e_{mech}(x) - e_{fluid}(x) = -\frac{\varepsilon V^2}{2(g-x)} + \frac{k_{mech}x^2}{2} + p_{fluid}x \quad (7)$$

Here, kinetic energy terms are ignored for simplifying the analysis. The stored potential energy as function of the valve displacement for $V < V_{pi}$ is shown in Figure 2. A stable valve position at small valve displacement is found ($de_{tot}/dx = 0$ and $d^2e_{tot}/dx^2 > 0$).

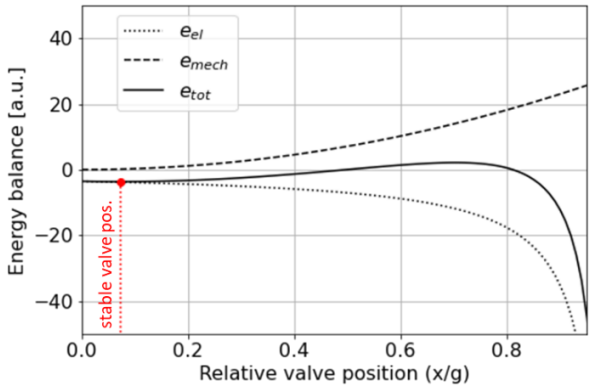

Figure 2: Energy balance of electrostatic valve structure for $V < V_{pi}$

Figure 3 compares the situation for different applied voltages (solid lines; $V_1 < V_{pi} < V_2$). When no voltage is applied ($V = 0$V), the stiffness of the system is $\sim k_{mech}$ for small displacements δx. For V > 0V, the stored energy e_{tot} will tend to $-\infty$ for $x/g \rightarrow 1$ (small effective gap). This occurs when the applied voltage is larger than V_{pi} or when the membrane dynamically overshoots beyond a critical displacement. In finite-elements, a proper contact model needs to be introduced to predict the collapsed shape of the membrane. The case for the pure penalty method is depicted in Figure 3.a (dashed lines; for illustrative purposes, the onset of the contact force is set for gaps smaller than $0.15g$). For a fixed contact stiffness k_p, the pure penalty method is effective for a certain range of voltages. In Figure 3.a, the contact stiffness k_p is chosen such that a stable position could be found for voltages a bit higher than V_{pi} (green line). If the applied voltage is further increased (red line), the contact force can no longer overcome the electrostatic pulling force and the model becomes unstable. A solution would be to increase the contact stiffness k_p, but if too high, the model becomes ill-conditioned, causing oscillatory behavior of the solver and/or inverted mesh elements.

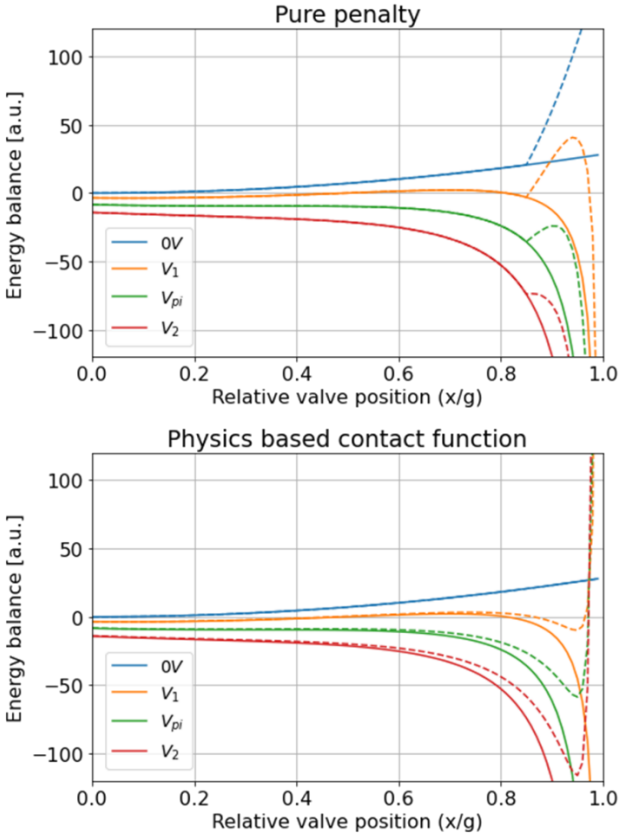

Figure 3: Comparison of (a) pure penalty and (b) physics-based contact function ($V_2 > V_{pi} > V_1$; solid lines= e_{tot} ; dashed lines = $e_{tot} + e_{contact}$)

The rationale of the physics-based contact function is to introduce a counteracting force such that the stability of the electro-mechanical system is restored:

$$t_{np} = \alpha \frac{k_p}{(g-x)^{n+2}} \quad (8)$$

with the exponent $n \geq 1$ and the pre-factor $\alpha > 0$.

During simulation, the initial boundary stiffness k_p was set to $\varepsilon V^2 g^n$. The advantage of this contact method compared to pure penalty is that it is an internal boundary method as shown by the dashed lines (n = 1; α = 0.025) in Figure 3.b, avoiding convergence issues. The pre-factor α is a continuation parameter. The model will steadily converge to a sufficiently accurate solution by scaling the pre-factor α, as illustrated in Figure 4.

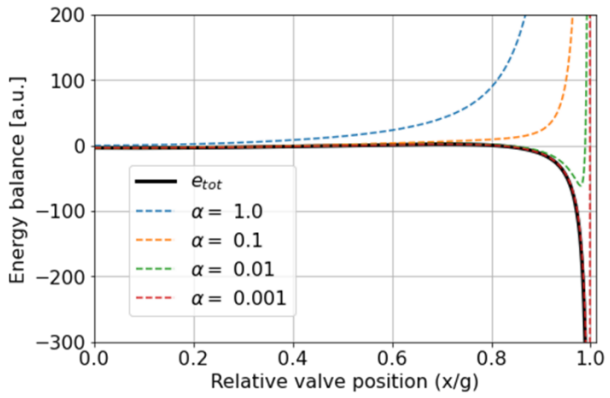

Figure 4: Physics-based contact function for different values of the continuation parameter α (dashed lines = $e_{tot} + e_{contact}$)

3. Steady state axisymmetric finite-element model

The axisymmetric valve model implemented in Comsol Multiphysics [6] is shown in Figure 5. The electrostatic valve consists of a flexible circular membrane (radii from 100 to 500 µm; thickness = 5 µm; E = 10 MPa; ν = 0.49) with a continuous, infinitely thin conductive film at the bottom. The ground electrode is covered with 500 nm nitride for electrical isolation ($\varepsilon_{r,nitride}$ = 7). Above the membrane and inside the valve cavity, dry air at standard temperature and pressure is assumed ($\varepsilon_{r,air} \sim 1$).

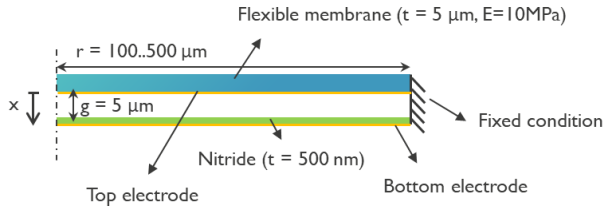

Figure 5: Axisymmetric circular valve structure

To illustrate the effectiveness of the physics-based contact function, a voltage of 100 V was applied over the valve electrodes of the circular membrane with a radius of 200 µm, well above its pull-in voltage of 20 V. The parameters n and k_p of the contact function were set to 2 and $\varepsilon V^2 g^2$. The pre-factor α was set as a continuation parameter in the solver and was swept from 1 to 10^{-10} in 100 logarithmic distributed steps. The initial values for the variables solved for in each step were taken equal to the solution of the previous step. Figure 6 depicts the effect of the continuation parameter α on the shape of the membrane collapsed on the ground electrode. The solution at $\alpha=10^{-10}$ was assumed converged by monitoring the area of the membrane in contact. Note that the contact function was offset 100 nm from the bottom nitride insulator to leave room for the moving mesh of the collapsing fluidic domain in the valve cavity. Values smaller than 100 nm let to numerical instabilities due to a degraded quality factor of particular elements in the fluid mesh.

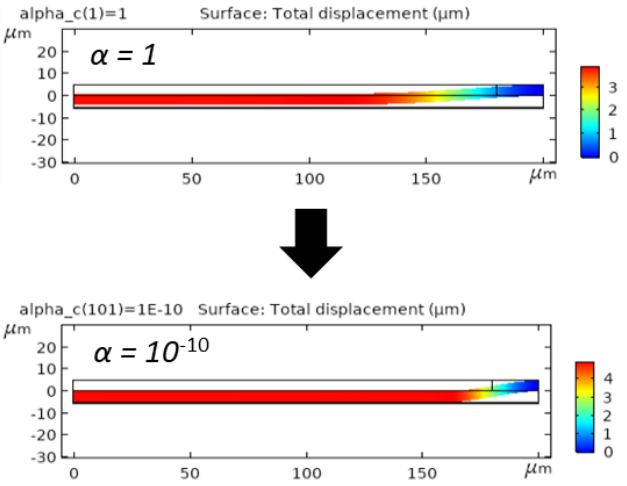

Figure 6: Circular membrane collapsed on ground electrode after pull-in: effect of the continuation parameter α (n = 2; $k_p = \varepsilon V^2 g^2$; V = 100 V; V_{pi} = 20 V; color scale in microns)

By repeating the above-described methodology for different initial voltages, the voltage-displacement curve could be obtained as shown in Figure 7. The pull-in occurring at 79.5 V is clearly visible, in this case for a membrane with a radius of 100 µm. The simulated static pull-in voltages for different membrane radii from 100 to 500 µm are depicted in Figure 8 and fit well with two nonlinear analytical models found in literature [7,8].

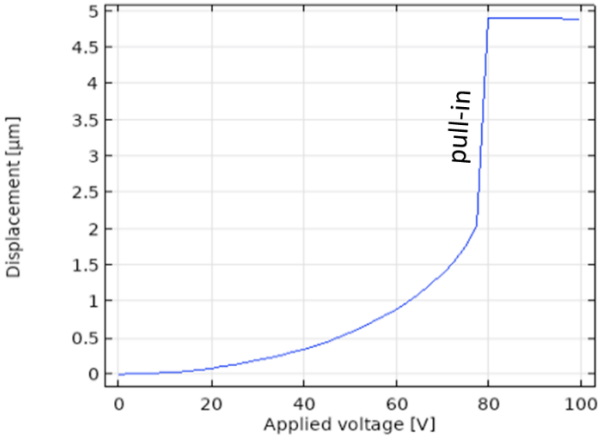

Figure 7: Voltage-displacement curve for a circular membrane with a radius of 100 µm (the displacement is probed at the membrane center)

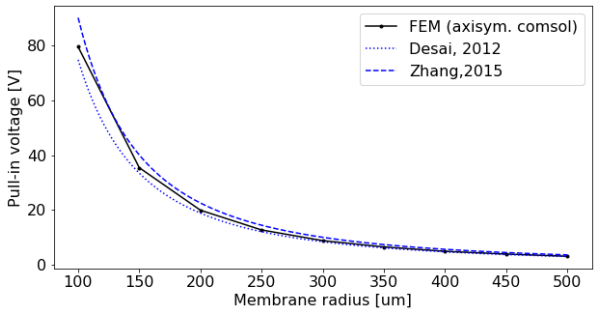

Figure 8: Effect of membrane size on the static pull-in voltage

The contact model can be extended to non-uniform electrostatic gaps by replacing the displacement x in Eq. (8) with the closest distance D to the ground electrode as found by solving the Eikonal equation:

$$|\nabla D| = 1 \qquad (9)$$

$D = 0$ on the ground electrode. $\nabla D.n = 0$ on all other boundaries with n the surface normal. The solutions for parabolic and Bezier curved bottom electrodes are shown in Figure 9.

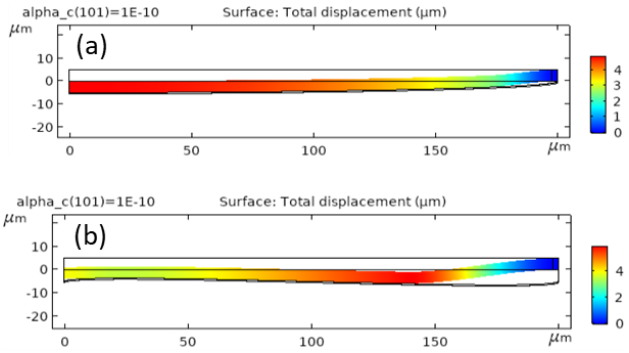

Figure 9: Electrostatic pull-in on (a) parabolic and (b) Bezier curved bottom electrodes (color scale in microns)

4. Transient fluid-structure interaction model

The physics-based contact function was next applied to the full electrostatic valve structure with a net air flow present in the air channel in the initial open position. The results of the transient fluid-structure interaction model are shown in Figure 10. The valve membrane had a radius of 250 μm. The other dimensions (membrane thickness and valve cavity) are the same as indicated in Figure 5. The gas inlet and outlet channel had a length, width, and height of respectively 250, 100 and 5 μm.

First an air pressure of 100 Pa was applied at the inlet, realizing an air flow of 0.4 μL/min through the channel as shown in Figure 10.b (assuming incompressible, no slip flow). Next the voltage was ramped to 30 V in 200 ms. Transient pull-in occurred around 24 V (see Figure 10.c). The transient pull-in voltage was higher than the static pull-in value of 12.5 V obtained in the axisymmetric model, because of the air flow in the microchannel. A surge in the air flux, both at the inlet and outlet boundaries was noticed during the pull-in event (see Figure 10.b). In the closed condition, the net flow rate was reduced twofold compared to the open condition. Finally, the voltage was ramped down to 0 V. Snap-out took place at a lower voltage, i.e. 15 V. As the membrane was in the collapsed position after the voltage up-ramp, the electrostatic force at the start of the voltage down-ramping was obviously higher. This transient voltage hysteresis between pull-in (voltage up-ramping) and snap out (voltage down-ramping) is clearly observed in Figure 10.c. The snap-out event was noted to be less abrupt, i.e. lower peak flow rates, with respect to pull-in.

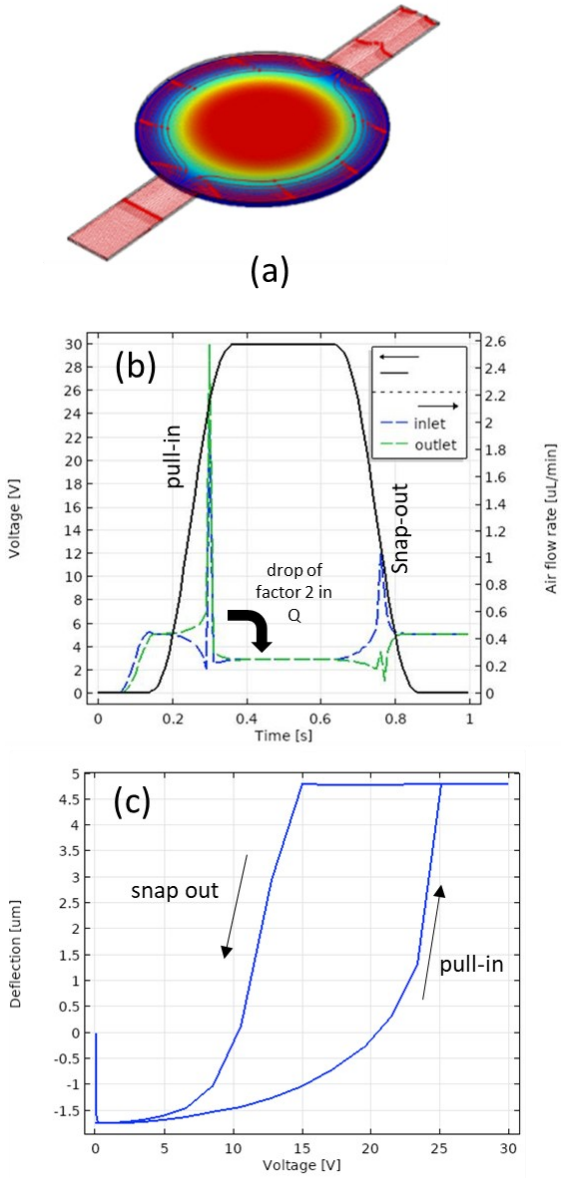

Figure 10: (a) Streamlines of the gas flow for the membrane in the collapsed state; (b) Transient change of the inlet/outlet air flux during one open/close cycle of the valve; (c) Voltage-displacement relationship of one valve open/close cycle (probed at the membrane center)

5. Conclusions

A convenient physics-based contact method was demonstrated for the transient modeling of an electrostatic actuated, gas modulating microvalve. The method can easily be extended to other electrostatic micro-actuators or sensors. More complex valve structures (curved electrodes) can be addressed by solving the Eikonal equation. By tuning the boundary conditions in the fluidic domain, the study of the transient behavior of the valve in a larger fluidic circuit is now conceivable, where issues such as crosstalk, variable delays and time dependent pressure levels need to be tackled.

References

1. Lau, A. T. H. *et al*, "Dynamics of microvalve operations in integrated microfluidics," *Micromachines*, Vol. 5 (2014), pp. 50-65
2. Eriksson, A, "Mechanical Model of Electrostatically Actuated Shunt Switch." *Proceedings of the COMSOL Multiphysics User's Conference*. 2005.
3. Pennec, F., et al. "Verification of contact modeling with COMSOL multiphysics software." Rapport LAAS n°07604 (2007).
4. Timoshenko, S. and Woinowsky-Krieger, S, Theory of Plates and Shells, McGraw-Hill Education (1959), pp. 55-56.
5. Rochus, V. *et al*, "Electrostatic coupling of MEMS structures: transient simulations and dynamic pull-in," *Nonlinear Analysis: Theory, Methods & Applications*, Vol. 63, No. 5-7 (2005), pp. 1619-1633.
6. COMSOL Multiphysics® v. 5.4. www.comsol.com. COMSOL AB, Stockholm, Sweden.
7. Desai, A. V. *et al*, "Design considerations for electrostatic microvalves with applications in poly (dimethylsiloxane)-based microfluidics," *Lab on a Chip*, Vol. 12, No. 6 (2012), pp. 1078-1088.
8. Zhang, W. *et al*, "Pull-in analysis of the flat circular CMUT cell featuring sealed cavity," *Mathematical Problems in Engineering*, Vol. 2015 (2015), Article ID 150279, 9 pages.